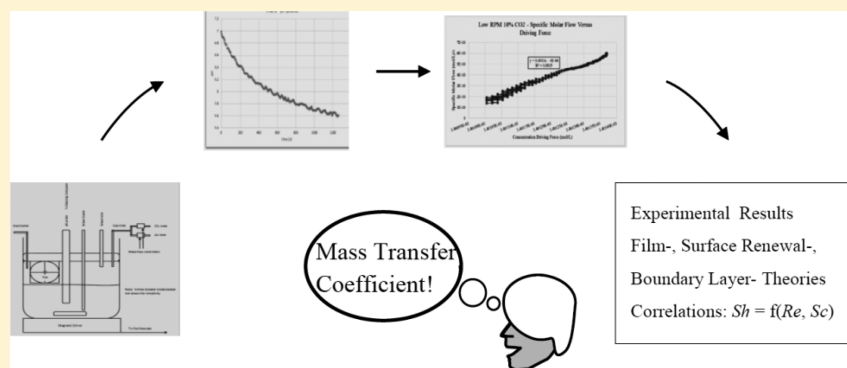


Facilitating Conceptual Understanding of Gas–Liquid Mass Transfer Coefficient through a Simple Experiment Involving Dissolution of Carbon Dioxide in Water in a Surface Aeration Reactor

Vivek P. Utgikar* and David MacPherson

Department of Chemical and Materials Engineering, University of Idaho, Moscow, Idaho 83844, United States

S Supporting Information



ABSTRACT: Students in the undergraduate *transport phenomena* courses typically have a greater difficulty in understanding the theoretical concepts underlying the mass transport phenomena as compared to the concepts of momentum and energy transport. An experiment based on dissolution of carbon dioxide in water was added to the course syllabus to facilitate the student learning of these concepts. A surface aeration reactor (SAR) with precisely defined interfacial area was designed for conducting the experiment. The students learned to setup and run the experiment, perform data analysis and communicate the results through written report and oral question-and-answer sessions. The students compared the experimentally observed values of the mass transfer coefficient with those predicted from correlations available in the literature. The hands-on experience enabled the students to relate the theoretical concepts covered in the lectures and textbooks to a real system. The students acquired a deeper understanding of the fundamental theories of mass transport and developed an appreciation for the significance of the mass transfer coefficient.

KEYWORDS: Upper Division Undergraduate, Laboratory Instruction, Physical Chemistry, Hands-On Learning, Transport Properties, Kinetics

Transport Phenomena courses involve a unified treatment of phenomena associated with momentum, energy, and mass transport, based on a “first-principles molecular or microscopic analysis” approach.^{1–3} This treatment involves conducting a balance over a fixed volume to express the accumulation of the quantity of interest (momentum, energy, or mass) as the difference between inflow, outflow, and the rate of generation or loss in that volume.⁴ Transport phenomena courses are required components of most undergraduate chemical engineering degree programs, and the discussion of the three transport phenomena is often included in advanced physical chemistry topics.^{4–7}

Typically, a student will have been exposed to concepts of momentum and energy transport through courses in fluid mechanics and heat transfer (frequently as a part of the engineering thermodynamics course) that often are prerequisites for the *transport phenomena* courses. However, no such prerequisite or foundation course exists for mass transfer, and the student has more difficulty in grasping the concepts of mass

transport phenomena as compared to the concepts of momentum and energy transport.

Transport phenomena courses are highly mathematical and intensively theoretical. The comprehension of the difficult concepts of the transport phenomena can be facilitated by introducing an experimental component in the course. An experiment can not only aid the students grasp the concepts but also teach them to analyze and synthesize data, acquire communication skills and develop partnership/teamwork practices.⁸ The experiment described in this paper was developed for the students in the third year (junior class) of the undergraduate chemical engineering program in order to enhance their understanding of the concept of the mass transfer coefficients in a gas–liquid system. The experiment involves

Received: November 3, 2015

Revised: April 18, 2016

determination of the flux of carbon dioxide into water through monitoring of the pH of the solution and relating it to the driving force for the mass transfer through the mass transfer coefficient. The theoretical principles underlying the experiment are described first followed by the experimental setup, procedure, results, and the analysis of the impact of the experiment in facilitating student learning of the mass transport phenomena concepts.

■ GAS–LIQUID MASS TRANSFER IN CO₂–WATER SYSTEM: THEORETICAL PRINCIPLES

The pressure and concentration profiles of component A, which is being transferred from the gas phase to the liquid phase, are shown in Figure 1.⁹ N_A is the flux (moles of A

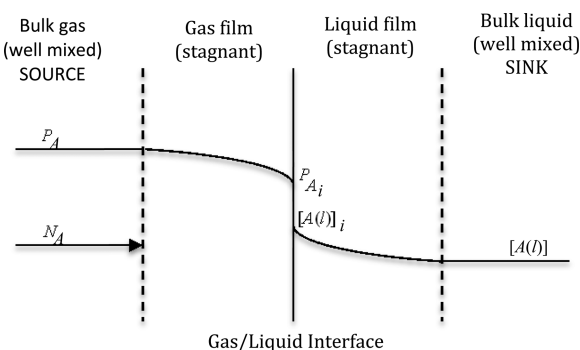


Figure 1. Mass transfer of A from gas to liquid phase: pressure and concentration profile (adapted from ref 9).

transferring from the gas to the liquid phase per unit time per unit area) of A, P_A and P_{A_i} are the partial pressures of A in the bulk gas phase and at the gas–liquid interface, respectively, and $[A(l)]$ and $[A(l)]_i$ are the bulk-liquid phase and interfacial concentrations, respectively.

The flux N_A can be expressed by several alternate equations involving different combinations of pressures and concentrations⁹

$$\begin{aligned} N_A &= k_G(P_A - P_{A_i}) = k_L([A(l)]_i - [A(l)]) \\ &= K_L([A(l)]^* - [A(l)]) \end{aligned} \quad (1)$$

where

- k_G : gas-side mass transfer coefficient
- k_L : liquid-side mass transfer coefficient
- K_L : overall liquid-side mass transfer coefficient based on the liquid side
- $[A(l)]^*$: hypothetical concentration of dissolved A in the liquid phase that would be in equilibrium with the partial pressure of A, P_A , in the gas phase

It should be noted that the interface is always assumed to be at equilibrium, that is, P_{A_i} is related to $[A(l)]_i$ through the equilibrium relationship. The overall mass transfer coefficient is obtained from the individual gas- and liquid-side mass transfer coefficients by⁹

$$\frac{1}{K_L} = \frac{1}{mk_G} + \frac{1}{k_L} \quad (2)$$

where m is the generalized equilibrium constant describing the relationship between the gas and liquid phases for A (usually Henry's law).

Applying these principles to CO₂ dissolution in water, N_{CO_2} , the molar flux of CO₂ from the gas to aqueous phase is given by

$$N_{CO_2} = K_L([\text{CO}_2(\text{aq})]^* - [\text{CO}_2(\text{aq})]) \quad (3)$$

where $[\text{CO}_2(\text{aq})]^*$ is the concentration of dissolved CO₂ in the aqueous phase that would be in equilibrium with the partial pressure of CO₂, P_{CO_2} , in the gas phase; and $[\text{CO}_2(\text{aq})]$ is the actual concentration of dissolved CO₂ in the aqueous phase.

Neglecting any nonidealities, $[\text{CO}_2(\text{aq})]^*$ is obtained from the equilibrium relationship for CO₂ in gas–aqueous solution as described by Henry's law¹⁰

$$[\text{CO}_2(\text{aq})]^* = P_{CO_2}/H_{CO_2} \quad (4)$$

where H_{CO_2} is the Henry's law constant for CO₂–water system, expressed in [pressure/concentration] units, atm/(kmol/m³), for example. (These units differ from the pressure units of the constant expected in the fundamental expression of Henry's law, which relates gas phase fugacity to mole fraction in the liquid phase, due to the liquid phase concentration being expressed in kmol/m³).

The CO₂ dissolved in the liquid phase immediately gets distributed into various molecular (carbonic acid/dissolved CO₂) and ionic species (bicarbonate and carbonate), and the CO₂ material balance for the liquid phase yields the following equation:

$$\frac{d[\text{CO}_2]_{\text{Tot}}}{dt} = K_L([\text{CO}_2(\text{aq})]^* - [\text{CO}_2(\text{aq})]) \cdot A_i/V \quad (5)$$

where

- A_i : interfacial area for mass transfer
- $[\text{CO}_2]_{\text{Tot}}$: total CO₂ concentration in the liquid including all molecular and ionic species
- V : volume of the liquid phase

The dissolved CO₂ (molecular species) and total CO₂ (molecular + ionic species) can be calculated from the pH of the solution (the details of the derivation are presented in the associated content)¹¹

$$[\text{CO}_2(\text{aq})] = \frac{10^{-2\text{pH}} - K_W}{K_1 + 2K_1K_2/10^{-\text{pH}}} \quad (6)$$

$$[\text{CO}_2]_{\text{Tot}} = \frac{10^{-2\text{pH}} - K_W}{K_1 + 2K_1K_2/10^{-\text{pH}}} \left(1 + \frac{K_1}{10^{-\text{pH}}} + \frac{K_1K_2}{10^{-2\text{pH}}} \right) \quad (7)$$

where

- K_1 : first ionization constant for carbonic acid
- K_2 : second ionization constant for carbonic acid
- K_W : ion product of water

The rate of dissolution of CO₂ in water can be monitored by simply measuring the pH of the system. If the system has a precisely defined interfacial area that can be determined accurately, the mass transfer coefficient for the system can be easily calculated from eq 5.

When the experiment is conducted with pure CO₂ in the gas phase, the overall mass transfer coefficient K_L is the same as the liquid side mass transfer coefficient k_L . The gas-side mass transfer coefficient k_G can then be determined by conducting the experiment under identical conditions, but with a CO₂–air mixture in the gas phase instead of pure CO₂.

Mathematically, for pure CO₂

$$k_L = K_L \quad (8)$$

and, for CO₂–air mixture

$$k_G = \frac{1}{H_{\text{CO}_2} \left(\frac{1}{K_L} - \frac{1}{k_L} \right)^{-1}} \quad (9)$$

Thus, a simple apparatus that involves a continuous monitoring and recording of the solution pH will yield the data required for the determination of both k_L and k_G . Equations 6 and (7) yield the values of the concentrations of dissolved CO₂ (molecular species) and total CO₂ (including all species), respectively. [CO₂(aq)]* is calculated from the partial pressure of CO₂ and Henry's constant (which is known for CO₂–water system) using eq 4, leaving the mass transfer coefficient K_L as the only known to be determined using eq 5. The individual mass transfer coefficient k_L and k_G can then be determined using eqs 8 and 9, respectively.

MATERIALS AND METHODS

The laboratory assignment statement, the experimental apparatus and the procedure are described below.

Assignment Statement

The salient features of the laboratory assignment handed to the students were:

- A concise statement of objectives and expected outcomes. Students were required not only to determine the parameters experimentally but also to compare their results with theoretical predictions.
- Clear delineation of submissions/deliverables from the students. The required components of the prelab and lab report were listed along with the maximum credits for each component.
- An oral report and examination of students, wherein they were required to explain their data and results and answer any questions the examiner may have.

Each group consisted of three students, and the prelab and laboratory reports were evaluated as a collective submission. The prelab report was due 1 week after assigning the experiment. Groups with a satisfactory prelab report were allowed to conduct the experiment over the next week. Laboratory reports were due 1 week after completion of the experiment, and the oral examinations were scheduled in the same week.

Experimental Setup: A Surface Aeration Reactor

The key requirements for a gas–liquid contactor are

1. Piping connections for continuous flow of the gas phase
2. Piping connections for filling and emptying the liquid phase
3. Mechanisms for ensuring mixing in each phase
4. Port for a pH probe to enable pH measurement, and cable connections for continuous recording of the pH data
5. A vortex-breaking mechanism for ensuring a constant interfacial area between the two phases

A surface aeration reactor (SAR) satisfying these requirements was designed in the laboratory and is shown in Figure 2 (schematic and photo).

The mixing in the gas phase was accomplished by means of a small fan placed in the headspace, whereas a magnetic stir-bar was used for mixing of the liquid phase. The vortex-breaking

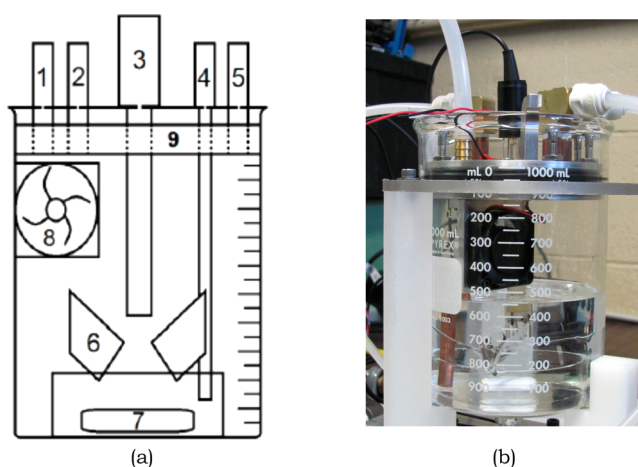


Figure 2. Surface aeration reactor: (a) schematic; (b) photo. (1, gas inlet; 2, water inlet; 3, pH probe; 4, solution outlet; 5, gas outlet; 6, vortex breaker; 7, magnetic stir bar; 8, fan; 9, beaker lid).

glass insert, shown in Figure 3, was extremely effective in maintaining a flat gas–liquid interface through the entire range

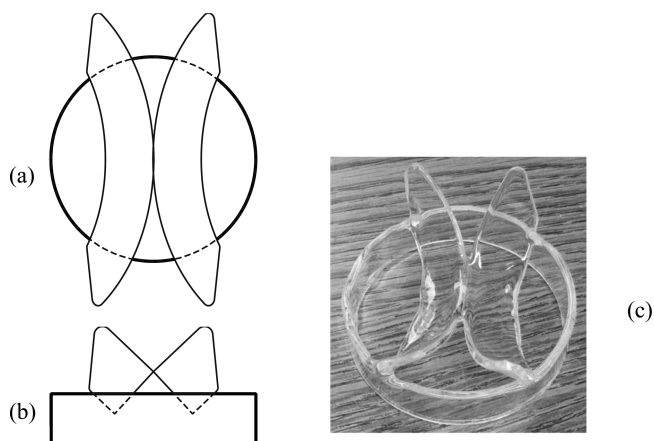


Figure 3. Vortex breaker: (a) top view, (b) front view, (c) photo.

of the stirring speeds. The pH of the system was monitored by a probe, with the data collected at a frequency of 0.5 Hz and recorded automatically. The rotational speed of the 1 in. long stir-bar was determined exactly by means of an oscilloscope and a pickup coil mounted inside the stir plate. Detailed information about system components is available in the Associated Content.

Experimental Procedure

The experimental procedure consisted of the following steps:

1. The SAR was filled up to approximately half its volume (~500 mL) with water and the volume noted.
2. With the stirring in the liquid phase off, pure CO₂ flow was started to the SAR, with the headspace fan turned on.
3. Sufficient time was allowed (~5–8 residence times based on headspace volume and gas flow) to flush out any residual air present initially in the reactor. The headspace can be assumed to consist of pure CO₂ at this time.
4. The liquid phase stirring was initiated at this point, with low stirring speed (~4 rps or 240 rpm).

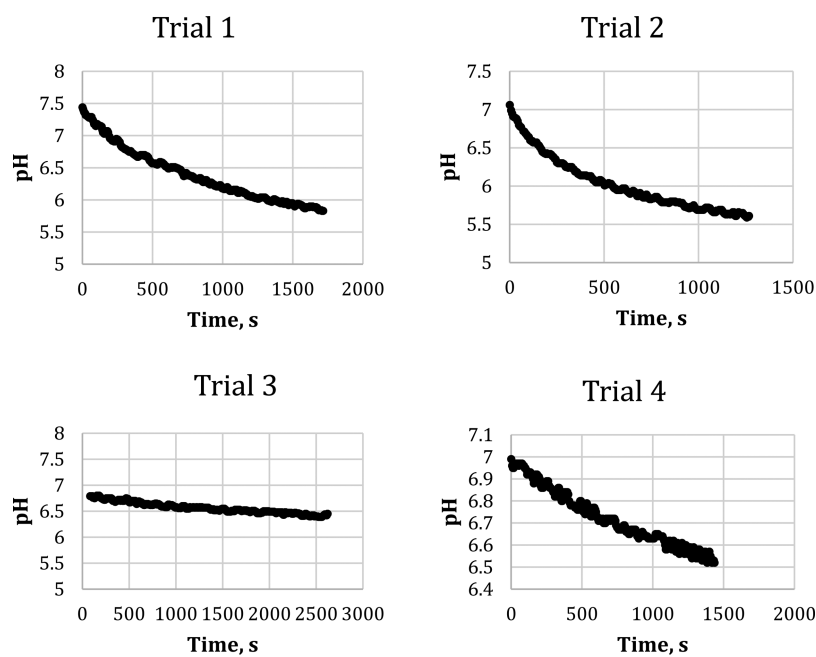


Figure 4. pH–time profiles. Trial 1: Pure CO₂, low rpm. Trial 2: Pure CO₂, high rpm. Trial 3: Air–10% CO₂ mixture, low rpm. Trial 4: Air–10% CO₂ mixture, high rpm.

- The continual recording of the pH was initiated and the data recorded for ~30–45 min.
- The experimental run was stopped by stopping the liquid phase stirring and recording of the pH data.
- The outlet valve on the gas line was closed, resulting in the emptying of the reactor of water due to CO₂ pressure.
- The gas outlet valve was opened and the reactor filled with fresh water.
- The above steps were repeated for a higher stirring speed (up to 20 rps or 1200 rpm).
- After completing the runs with pure CO₂, data were collected for 10% CO₂–air mixture at the same stirring speeds as for pure CO₂ by repeating the above steps. The composition of the gas stream was maintained constant by means of the two mass flow controllers, which ensured the constant proportion between the air and CO₂ flow rates.

Details regarding the materials and methods is available in the [Supporting Information](#).

HAZARDS

The materials used in the experiment pose little hazard to human health and environment: CO₂ is inert and has very low toxicity, and the liquid phase consists of water. Nevertheless, certain basic safety precautions need to be observed: the compressed gas cylinders must be securely fastened to the wall or bench, and proper regulators/valves/piping must be used for manipulating and controlling the flow. The experiment should be conducted in adequately ventilated area to avoid any potential asphyxiation situation in case of buildup of CO₂. Lastly, excessive buildup of pressure in the SAR during draining of water can cause the glass beaker to shatter, potentially causing injury. This situation can be easily prevented by avoiding overpressurizing of the SAR.

RESULTS AND DISCUSSION

Experimental Observations and Data Analysis

As mentioned above, each group conducted four runs: two with pure CO₂ at low and high stirring speeds, and two with air–10% CO₂ mixture at the same stirring speeds as in the runs with pure CO₂. Typical pH–time data recorded by one of the groups for its four runs are shown in [Figure 4](#). The following observations could be generalized across almost all groups:

- The pH of the solution decreased continuously in all runs and did not show any signs of leveling off.
- The rate of pH decrease was lower at the lower stirring speed for both pure CO₂ and air–10% CO₂ systems.
- Systems with pure CO₂ exhibited higher rate of decrease than air–10% CO₂ systems at the same stirring speed.
- The highest rate of pH decrease was observed for pure CO₂ at the higher stirring speed, whereas the lowest rate of decrease was observed for air–10% CO₂ mixture at the lower stirring speed.

The initial high pH observed in the experiments can be attributed to the source of water supply, groundwater from the deep basaltic Grand Ronde Aquifer. The chemical evolution of groundwater in such aquifers is influenced by two major processes occurring with the precipitation and other surface waters (that are oxygenated, weakly acidic, and CO₂ charged) infiltrating the aquifer: (1) dissolution of basalt by carbonic acid and (2) silicate hydrolysis. The progressive silicate hydrolysis and dissolution result in an increase in the silicate content and the pH from 7 to as high as 10 in some locations.¹²

These data, which were recorded in a data file, were then typically imported into a spreadsheet program by the groups. The dissolved molecular CO₂ and total CO₂ concentrations were then computed from the pH values using [eqs 6 and 7](#), respectively. Estimating the mass transfer coefficient K_L from [eq 5](#) requires calculation of the time derivative of $[\text{CO}_2]_{\text{Tot}}$. All the groups used regression analysis to fit a polynomial to the $[\text{CO}_2]_{\text{Tot}}$ –time data, typically with high regression coefficients

values >0.9 . The left-hand side of eq 5, $\frac{d[\text{CO}_2]_{\text{Tot}}}{dt}$, was then obtained by simply differentiating this polynomial expression. The overall mass transfer coefficient based on the liquid side, K_L , was then obtained by linear regression of $\frac{d[\text{CO}_2]_{\text{Tot}}}{dt}$ against $([\text{CO}_2(\text{aq})]^* - [\text{CO}_2(\text{aq})])$ as indicated by eq 5. Figure 5

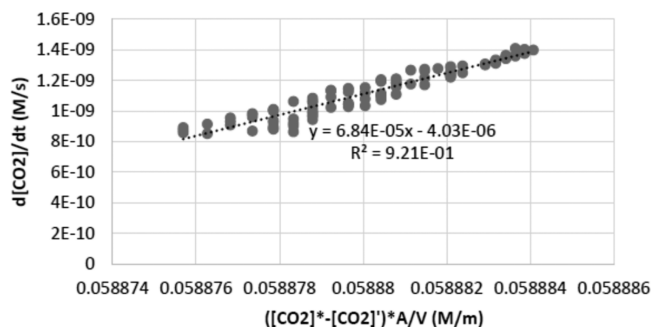


Figure 5. Example of regression of eq 3 for mass transfer coefficient estimation for air–10% CO_2 mixture at high stirring speed.

shows a typical regression plot obtained by one of the groups for the air–10% CO_2 mixture at the high stirring speed. The overall mass transfer coefficient in this run, as found out by the group was $6.85 \times 10^{-5} \pm 1.11 \times 10^{-6}$ m/s.

Numerical Results and Comparison with Theoretical Predictions

Different groups conducted the experiment at different rotational speed of the stir-bar ranging from 4 to 20 rps. There was considerable variation in the reported values of the mass transfer coefficients. The overall mass transfer coefficients (K_L) reported ranged from 4.0×10^{-7} m/s (low stirring speed, air–10% CO_2 mixture) to 3.0×10^{-5} m/s (high stirring speed, pure CO_2). The experimental results indicated that

1. The individual liquid-side mass transfer coefficient values (k_L) ranged from $\sim 8.0 \times 10^{-7}$ m/s to 1.0×10^{-5} m/s.
2. The values of the individual gas-side mass transfer coefficient (k_G) were found to range from 3.9×10^{-3} – 2.5×10^{-2} mol/s m^2 atm.
3. The contribution of the gas-side resistance to the overall resistance varied widely, with a low of 15% at low stirring speed to a high of $\sim 90\%$ at high stirring speeds.
4. Increasing the stirring speed of the aqueous solution caused the liquid-side mass transfer coefficient to increase by a factor of 1.4–30.

The values reported by the different groups show considerable variation. These variations can be attributed to two causes—data acquisition errors and data processing errors. The data acquisition errors arise from nonadherence to rigorous procedure, and possible fluctuations in pH primarily due to the nature of the system—it is well-known that errors and fluctuations occur in pH measurements in low conductivity solutions.¹³ Instrument errors are also possible, though a rigorous calibration protocol followed makes it less likely. The errors in the acquired data could possibly be amplified in the data processing, where curve-fitting, differentiation and linear regression operations are conducted with the data. In particular, differentiation of uncertain data leads to instability¹⁴ and is possibly the single largest source of errors in the result.

The laboratory assignment statement required the groups to compare the experimentally obtained mass transfer coefficient

values with those predicted on the basis of correlations available in the literature. Several correlations have been reported in literature for the prediction of gas–liquid mass transport coefficients, though not for the specific system used in these experiments.¹⁵ The correlation reported by Versteeg et al.¹⁶ for SARs was used for comparison purposes based on the similarity of the systems

$$\text{Sh} = 0.064\text{Re}^{0.72}\text{Sc}^{0.5} \quad (10)$$

The dimensionless Sherwood, Reynolds, and Schmidt numbers are defined as

$$\text{Sh} = \frac{k_L d}{D_{AB}} \quad (11)$$

$$\text{Re} = \frac{d^2 N}{\nu} \quad (12)$$

$$\text{Sc} = \frac{\nu}{D_{AB}} \quad (13)$$

where

- d : diameter of the stirrer (length of the stir-bar)
- N : speed of revolution (rps)
- ν : kinematic viscosity
- D_{AB} : diffusivity of CO_2 in water

As mentioned above, the experimentally observed values of the mass transfer coefficient varied greatly, and the agreement between these observed values and those predicted using the correlation stated above varied widely as well. Typically, the discrepancy ranged from 10 to 50%, though in some cases the values differed by an order of magnitude. Considering the fact that the correlation has been developed for turbine-type impellers and not magnetic stirrers, such discrepancy was expected.

Communication of Results: Oral Examination

According to ABET, all engineering courses should be structured to promote in students the ability to communicate effectively. The prelab and laboratory report were group submissions and provided a measure of the group's written communication ability. However, it is difficult to determine from a group submission the contribution of the individual student, as well as his/her communication ability and the level of comprehension of the concepts of mass transport phenomena. Therefore, each student was subjected to a 15 min question-and-answer session, wherein his/her knowledge of the experiment and theoretical concepts was evaluated. Details of the evaluation basis are available in the associated content.

Most of the students displayed a good understanding of the speciation of CO_2 in water and the equilibria among the various species. It also became apparent that they understood the additivity of mass transport resistances on the gas and liquid side. Some of the students did experience difficulty in drawing a sketch of the concentration profile as a function of time. About 33% of the students initially sketched the profile with zero slope at the interface. However, with some helpful hints, they eventually could draw something resembling the classic similarity transform solution to the diffusion equation. At this point, they could relate the reduced flux to decreasing concentration gradient at the interface and its dependence upon the surface renewal rate. A few of the students answered these questions readily, allowing the evaluator to get into more

detailed discussions of the effect of the reactions on the CO₂ concentration profile. The average and median scores on the oral portion of the report were ~76%, with a standard deviation of 15%. The maximum and minimum scores were 96% and 52%, respectively, and the mode was 92%. The overall statistics for the experiment including the prelab and laboratory report were as follows: average and median, 82%; standard deviation, 9%; maximum, 97%; minimum, 64%; and mode, 85%. The high level of anxiety in some students due to their lack of familiarity/earlier exposure to oral examination was one of the factors contributing to lower score on the oral assessment portion of the laboratory.

Pedagogical Lessons

The goal behind the development and incorporation of this experiment in the *Transport Phenomena* course was to increase the level of understanding of the complex mass transport phenomena concepts in the students. The majority of the students were able to conduct the experiment, analyze data, and derive necessary mass transfer coefficient values and relate those to the theory.

One of the groups also used the film theory and the boundary-layer theory to obtain estimates of the mass transfer coefficient. The film theory predicts a linear dependence of the mass transfer coefficient on the diffusivity, whereas the boundary-layer theory predicts a dependence on $D_{AB}^{2/3}$.⁹ The group compared the numbers and inferred that the surface-renewal theory, which predicts a dependence on the square-root of diffusivity, described the mass transfer process more accurately than the other two theories.

Overall, the experiment was viewed as being very helpful in promoting interest in and explaining the concepts of transport phenomena. The student feedback indicated that it taught them how to apply formulas and relationships to real world data and observations.

Future Modifications

This experiment is similar to the one described by Hill⁶ who employed pH measurements in a sparged gas reactor to determine the *volumetric* mass transfer coefficients. Systems other than CO₂–water have also been employed to study and obtain the volumetric mass transfer coefficient.¹⁷ The advantage of using a SAR is that the interfacial area is defined precisely, and the parameter obtained is the mass transfer coefficient, which the students can relate to the theoretical concepts of the mass flux, the essential foundation of the mass transport phenomena discussion. The estimation of interfacial area in a sparged reactor introduces an additional empirical component that may sometimes detract from the transport phenomena theory. SAR is also preferable to other contacting devices such as packed columns or bubble columns, where gas holdup and interfacial area estimations can introduce additional uncertainty.^{18,19} pH measurements offer a highly convenient, instantaneous technique to monitor the progress of the system. Pantaleão et al.²⁰ describe a carbon dioxide sorption experiment in a membrane contactor, where visual inspection of the color change in the system provides a qualitative measure, however, the quantitative measurement required use of infrared analyzer making the system more complex overall.

Future improvements to the experiments will include obtaining data over a wider range of stirring speeds so that a more accurate correlation of the form ($Sh = cRe^m Sc^n$) can be developed for this system. This will be accomplished by assigning specific rotational speeds to different groups, as a

typical run takes about 30 min to run, and a group is only able to conduct 4–5 runs in the time available for the experiment. In addition, the rotational speed of the fan in the gas headspace will also be varied, allowing a development of a correlation for the gas-side mass transfer coefficient, k_G . The data obtained from all groups will then be shared but analyzed separately by each group.

The second modification will involve increased theoretical analysis of the data using the three different theories: the film-theory, the surface-renewal theory, and the boundary-layer theory, as done by one of the groups. This will help the students relate the theory, which they often find too abstract, to experimental observations and real data improving the understanding of the transport phenomena concepts.

The third modification will involve improving the accuracy of measurements by manipulating the ionic strength of the solution by adding salts to obtain more stable pH measurements. As mentioned above, pH measurements in low conductivity systems are subject to greater fluctuations that introduce errors in the data collection and analysis. Such errors will be minimized in future experiments.

Further, the analysis of the data will be refined to increase the accuracy of estimates of the derivative, $\frac{d[CO_2]_{Tot}}{dt}$. The analysis described in this paper involved fitting a polynomial expression for the entire range of the $[CO_2]_{Tot}$ versus time data, and then differentiating that expression analytically. However, it is likely that a single polynomial expression may not describe the relationship between the total CO₂ concentration and time with sufficient accuracy over the entire time period. As mentioned above, any data errors are amplified in differentiation. Therefore, to increase the accuracy of estimate of the derivative at any point, a local data set will be considered and regression carried out for this data set to obtain a polynomial expression that can describe these data more accurately. Thus, the entire data will be described by a series of polynomial expressions that are valid over only a portion of the data. This will lead to better estimates of $\frac{d[CO_2]_{Tot}}{dt}$, and hence of the mass transfer coefficients.

The teaching of the transport phenomena course must lead to students understanding the mathematical model to apply the principles of transport phenomena to engineering situations.²¹ Further, they must be trained to make correct assumptions to use adequately the transport equations and have clarity regarding the nature of the coefficients. The experiment described in this paper accomplishes that while developing the much-needed analysis, synthesis, teamwork, and communication skills in the students.

CONCLUSIONS

The carbon dioxide–water system is ideally suited for explaining the concept of mass transfer coefficient to undergraduate students of transport phenomena. The substances involved are easily available, have very low toxicity and present few hazards, and above all, the required data can be obtained through automated measurements of the system pH. The measured data can be easily manipulated, yielding necessary quantities for the determination of the overall, liquid-side, and gas-side mass-transfer coefficients. The incorporation of this experiment in the transport phenomena course was valuable in enhancing student understanding of the mass transport concepts. The students also learned how to

work in groups, participate in data analysis, contribute to a written report, and develop oral presentation skills. It is hoped that this hands-on exercise will reinforce the complex theoretical concepts of transport phenomena and result in a student body that is interested and engaged in the learning process.

■ ASSOCIATED CONTENT

📄 Supporting Information

The Supporting Information is available on the ACS Publications website at DOI: [10.1021/acs.jchemed.5b00882](https://doi.org/10.1021/acs.jchemed.5b00882).

Laboratory Assignment Statement, Experimental Setup and Procedure, Gas–Liquid Equilibrium and Concentration of Species in CO₂–Water System, Oral Presentation Evaluation Rubric, Pedagogical Lessons. (PDF)

Laboratory Assignment Statement, Experimental Setup and Procedure, Gas–Liquid Equilibrium and Concentration of Species in CO₂–Water System, Oral Presentation Evaluation Rubric, Pedagogical Lessons. (DOCX)

■ AUTHOR INFORMATION

Corresponding Author

*E-mail: vutgikar@uidaho.edu.

Notes

The authors declare no competing financial interest.

■ REFERENCES

- (1) Hill, M. Chemical product engineering – the third paradigm. *Comput. Chem. Eng.* **2009**, *33*, 947–953.
- (2) Heinänen, V.; Seuranen, T.; Hurme, M. Chemical engineering education and industry megatrends. *Proceedings of the 11th International Symposium on Process Systems Engineering*; Karimi, I. A., Srinivasan, R., Eds.; Elsevier: Amsterdam, 2012; 975–979.
- (3) Armstrong, R. C. R. Byron Bird: the integration of transport phenomena into chemical engineering. *AIChE J.* **2014**, *60*, 1219–1224.
- (4) Fink, J. K. *Physical Chemistry in Depth*; Springer-Verlag: Berlin/Heidelberg, Germany, 2009.
- (5) Jimenez-Estallar, L.; Guillen-Gosalbez, G.; Boer, D. T. What, if anything, is a chemical engineer? *Comput.-Aided Chem. Eng.* **2009**, *27*, 2121–2126.
- (6) Utgikar, V. P. Facilitating active learning of concepts in transport phenomena: experiment with a subliming solid. *Chem. Eng. Educ.* **2015**, *49* (4), 215–220.
- (7) Cañizares, P.; García-Gómez, J.; Fernández de Marcos, I.; Rodrigo, M. A.; Lobato, J. Measurement of mass-transfer coefficients by an electrochemical technique. *J. Chem. Educ.* **2006**, *83*, 1204–1207.
- (8) Miller, R. L.; Ely, J. F.; Baldwin, R. M.; Olds, B. M. Higher order thinking in a unit operations laboratory. *Chem. Eng. Educ.* **1998**, *32* (2), 146–151.
- (9) Welty, J.; Wicks, C. E.; Wilson, R. E.; Rorrer, G. L. *Fundamentals of Momentum, Heat and Mass Transfer*, 5th ed.; John Wiley: New York, NY, 2007.
- (10) Majer, V.; Sedlbauer, J.; Bergin, G. Henry's law constant and related coefficients for aqueous hydrocarbons, CO₂ and H₂S over a wide range of temperature and pressure. *Fluid Phase Equilib.* **2008**, *272*, 65–74.
- (11) Hill, G. A. Measurement of overall volumetric mass transfer coefficients for carbon-dioxide in a well-mixed reactor using a pH probe. *Ind. Eng. Chem. Res.* **2006**, *45*, 5796–5800.
- (12) Nelson, B. J.; Wood, S. A.; Osiensky, J. L. Rare earth element geochemistry of groundwater from Palouse Basin, northern Idaho-eastern Washington. *Geochem.: Explor., Environ., Anal.* **2004**, *4*, 227–241.
- (13) Ito, S.; Hachiya, H.; Baba, K.; Asano, Y.; Wada, H. Improvement of the silver/silver chloride reference electrode and its application to pH measurement. *Talanta* **1995**, *42*, 1685–1690.
- (14) Chapra, S. C.; Canale, R. P. *Numerical Methods for Engineers*, 6th ed.; McGraw-Hill: New York, NY, 2010.
- (15) Lemoine, R.; Fillion, B.; Behkish, A.; Smith, A. E.; Morsi, B. I. Prediction of gas-liquid volumetric mass transfer coefficients in surface-aeration and gas-inducing reactors using neural networks. *Chem. Eng. Process.* **2003**, *42*, 621–643.
- (16) Versteeg, G. F.; Blauwhoff, P. M. M.; van Swaaij, W. P. M. The effect of diffusivity on gas-liquid mass transfer in stirred vessels. Experiments at atmospheric and elevated pressures. *Chem. Eng. Sci.* **1987**, *42*, 1103–1119.
- (17) Zieverink, M. M. P.; Kreutzer, M. T.; Kapteijn, F.; Moulijn, J. A. Gas-liquid mass transfer in benchscale stirred tanks – fluid properties and critical impeller speed for gas induction. *Ind. Eng. Chem. Res.* **2006**, *45*, 4574–4581.
- (18) Murrieta, C. R.; Seibert, A. F.; Fair, J. R.; Rocha-U, J. A. Liquid-side mass-transfer resistance of structured packings. *Ind. Eng. Chem. Res.* **2004**, *43*, 7113–7120.
- (19) Akita, K.; Yoshida, F. Gas holdup and volumetric mass transfer coefficient in bubble columns. Effects of liquid properties. *Ind. Eng. Chem. Process Des. Dev.* **1973**, *12*, 76–80.
- (20) Pantaleão, I.; Portugal, A. F.; Mendes, A.; Gabriel, J. Carbon Dioxide Absorption in a Membrane Contactor with Color Change. *J. Chem. Educ.* **2010**, *87*, 1377–1379.
- (21) I&E C. I&EC Reports and Comments: Teaching transport phenomena. *Ind. Eng. Chem.* **1967**, *59* (9), 11–12. [10.1021/ie51403a004](https://doi.org/10.1021/ie51403a004).